

Preparation and characterization of copper nanoparticles of *Schisandra chinensis* and evaluation of its antiproliferative activity

Dario A. Tinjacá ^{1a*}, Ovidio A. Almanza ^{2b}, Felix Delgado ^{3c}, Sandra Johana Morantes ^{4d}, María C. Medina ^{1c}, Paola Torres ^{1f}, Estefanía Martínez ^{1g}

¹ Universidad El Bosque, Facultad de Ciencias, Química Farmacéutica, Grupo de Investigación en Química aplicada (INQA), Semillero de Investigación SIFUB, Bogotá D.C., Colombia.

² Universidad Nacional de Colombia, Facultad de Ciencias, Departamento de Física, Grupo de Física Aplicada, Bogotá D.C., Colombia.

³ Universidad El Bosque, Vicerrectoría de Investigaciones, Grupo de Virología, Bogotá D.C., Colombia.

⁴ Universidad El Bosque, Facultad de Ciencias, Programa Química Farmacéutica, Grupo de Investigación en Química Aplicada- INQA, Bogotá D.C., Colombia.

E-mail addresses: ^a dtinjacab@unbosque.edu.co, ^b oalmanzam@unal.edu.co,

^c delgadofelix@unbosque.edu.co, ^d smorantes@unbosque.edu.co, ^e mcmedina@unbosque.edu.co,

^f ptorresch@unbosque.edu.co, ^g emartinezqu@unbosque.edu.co

*Corresponding author.

Received: January 15, 2024

Corrected: February 6, 2024

Accepted: February 7, 2024

SUMMARY

Introduction: *Schisandra chinensis* is a plant species whose fruits have been well known for its multiple pharmacological effects. In the current work, aqueous extract of *S. chinensis* fruits is used to produce Copper nanoparticles (CuNPs) through green-synthesis method. Physical and biological essays characterized the nanoparticles obtained. **Aim:** To produce Copper nanoparticles through a green-synthesis method using the aqueous extract of *S. chinensis* fruits and to characterize this material using spectroscopic methods, including UV-Vis, FTIR (Fourier Transform Infrared Spectra), X-ray diffraction, and SEM (Scanning electron microscopy). Subsequently, the nanoparticulate material is evaluated against three tumor cell lines: A549 human lung cancer cell line (CRM-CCL-185TM), HT29 human colorectal adenocarcinoma cell line (ATCC® HTB-38TM) and MCF7 breast cancer cell line (ATCC® HTB-22TM). **Results:** Through a green-

synthesis method, Copper nanoparticles were synthesized from aqueous extract of *S. chinensis* fruits, demonstrating a spherical morphology with a size close to 26 nanometers by means of spectral methods. Furthermore, results suggest that the *S. chinensis* reduced CuNPs were able to induce mainly early apoptotic cell death in cancer cells in a concentration-dependent manner. **Conclusions:** The results proved that *S. chinensis* fruit aqueous extract could be applied for a greener synthesis of copper nanoparticles with potential anti-proliferative effect.

Keywords: *Schisandra chinensis*; material science; nanotechnology, green synthesis, copper nanoparticles, antiproliferative effects, carcinoma.

RESUMEN

preparación y caracterización de nanopartículas de cobre de *Schisandra chinensis* y evaluación de su actividad antiproliferativa

Introducción: *Schisandra chinensis* es una especie vegetal cuyos frutos han sido muy conocidos por sus múltiples efectos farmacológicos. En el trabajo actual, se utiliza extracto acuoso de frutos de *S. chinensis* para producir nanopartículas de cobre (CuNP) mediante el método de síntesis verde. Ensayos físicos y biológicos caracterizaron las nanopartículas obtenidas. **Objetivo:** producir nanopartículas de cobre mediante un método de síntesis verde utilizando el extracto acuoso de frutos de *S. chinensis* y caracterizar este material mediante métodos espectroscópicos, incluidos UV-Vis, FTIR (espectros infrarrojos por transformada de Fourier), difracción de rayos X y SEM. (Microscopía electrónica de barrido). Posteriormente, el material nanoparticulado se evalúa frente a tres líneas celulares tumorales: línea celular de cáncer de pulmón humano A549 (CRM-CCL-185TM), línea celular de adenocarcinoma colorrectal humano HT29 (ATCC® HTB-38TM) y línea celular de cáncer de mama MCF7 (ATCC® HTB -22TM). **Resultados:** Mediante un método de síntesis verde, se sintetizaron nanopartículas de cobre a partir de extracto acuoso de frutos de *S. chinensis*, demostrando mediante métodos espectrales una morfología esférica con un tamaño cercano a los 26 nanómetros. Además, los resultados sugieren que las CuNP reducidas de *S. chinensis* fueron capaces de inducir principalmente la muerte celular apoptótica temprana en células cancerosas de una manera dependiente de la concentración. **Conclusiones:** Los resultados demostraron que el extracto

acuoso del fruto de *S. chinensis* podría aplicarse para una síntesis más ecológica de nanopartículas de cobre con potencial efecto antiproliferativo.

Palabras clave: *Schisandra chinensis*; ciencia material; nanotecnología, síntesis verde, nanopartículas de cobre, efectos antiproliferativos, carcinoma.

RESUMO

Preparação e caracterização de nanopartículas de cobre de *Schisandra chinensis* e avaliação de sua atividade antiproliferativa

Introdução: *Schisandra chinensis* é uma espécie vegetal cujos frutos são bastante conhecidos por seus múltiplos efeitos farmacológicos. No presente trabalho, extrato aquoso de frutos de *S. chinensis* é utilizado para produzir nanopartículas de cobre (CuNPs) através do método de síntese verde. Ensaio físicos e biológicos caracterizaram as nanopartículas obtidas. **Objetivo:** Produzir nanopartículas de cobre através de um método de síntese verde usando o extrato aquoso de frutos de *S. chinensis* e caracterizar este material usando métodos espectroscópicos, incluindo UV-Vis, FTIR (Fourier Transform Infrared Spectra), difração de raios X e MEV. (Microscopia eletrônica de varredura). Posteriormente, o material nanoparticulado é avaliado contra três linhagens de células tumorais: linhagem celular de câncer de pulmão humano A549 (CRM-CCL-185TM), linhagem celular de adenocarcinoma colorretal humano HT29 (ATCC® HTB-38TM) e linhagem celular de câncer de mama MCF7 (ATCC® HTB-22TM). **Resultados:** Através de um método de síntese verde, nanopartículas de cobre foram sintetizadas a partir de extrato aquoso de frutos de *S. chinensis*, demonstrando uma morfologia esférica com tamanho próximo a 26 nanômetros por meio de métodos espectrais. Além disso, os resultados sugerem que os CuNPs reduzidos de *S. chinensis* foram capazes de induzir principalmente a morte celular apoptótica precoce em células cancerosas de uma maneira dependente da concentração. **Conclusões:** Os resultados provaram que o extrato aquoso da fruta *S. chinensis* pode ser aplicado para uma síntese mais verde de nanopartículas de cobre com potencial efeito antiproliferativo.

Palavras-chave: *Schisandra chinensis*; ciência dos materiais; nanotecnologia, síntese verde, nanopartículas de cobre, efeitos antiproliferativos, carcinoma.

INTRODUCTION

The application of nanoscale materials is an emerging area of pharmaceutical nanotechnology. Nanoparticles are structures with a size extending approximately from 1 nm up to 100 nm in length exhibiting specific characteristics in distribution and morphology [1]. Synthesis of copper nanoparticles (CuNPs) is interesting for the scientific community because of the wide range of applications in pharmaceuticals, photonics, electronics, sensing and catalysis [2, 3]. CuNPs have interest due to their excellent physical and chemical properties such as high surface-to-volume ratio, thermal conductivity, as well as their capacity to penetrate cellular barriers [4]. In fact, these nanoparticles could be used in cancer diagnosis and treatment [5]. The production of metallic CuNPs with different morphologies and sizes has been realized during the last decade by using different routes [6-13]. Although various techniques including chemical and physical procedures have been developed, an alternative route is the biosynthesis of metal nanoparticles starting from plant extracts [14, 15]. The last one is a specific application of green chemistry, characterized by a more efficient and less hazardous synthesis process, being a cost-effective and eco-friendly approach. Because the control of particle size and morphology are essential characteristics for application in biomedicine, the biological approach is superior to the chemical and physical synthesis methods for metal nanoparticles [16]. Such Likewise, stabilization of copper ions using leaf or fruit extracts and characterization of resulting nanoparticles have been documented in previous studies [17, 18].

The use of vegetable extracts for the biosynthesis of metal nanoparticles is based on the observation that plants can uptake and bio-reduce metal ions from soils and solutions. Many plant species contain different types of antioxidative compounds (reductant agents) such as flavonoids, coumarins, xanthenes, anthraquinones, and terpenoids. The phytochemical-enriched plant extracts are the principal ones involved in metal salt reduction from positive oxidation state to zero, and thus, acting as reducing agents. These substances, traditionally referred as secondary metabolites, are distributed differentially among limited taxonomic groups within the plants kingdom. For instance, a broad range of plants with high content of these metabolites, including *Allium sativum* [19], *Ocimum sanctum* L. [20], *Capparis spinose* [21], *Citrus limon* [22], *Curcuma longa* [23], *Magnolia Kobus* [24], *Passiflora foetida* [25], *Piper retrofractum* Vahl [26], *Punica granatum* [27], *Asparagus adscendens* [28], have been used for the synthesis of CuNPs. Furthermore, some studies revealed that using plant extracts as reductant agents for the synthesis of CuNPs by the biological method exhibited anticancer potential, antiproliferative and cytotoxic activity [29-32]. Another reports about synthesis of nanoparticles or composites using fruit extracts especially utilizing flavonoids, polyphenols etc. have been reported numerous times in the past [33, 34].

Schisandra chinensis is a plant species whose fruits have been well known in Far Eastern medicine for a long time. It had been reported that the most important components of the *S. chinensis* berries are dibenzo[a,c]cyclooctadiene lignans also known as “schisandra lignans” [35], which are not easily found in other plants. Lignans are secondary metabolites that belong to the polyphenolic compounds. Moreover, some studies demonstrated that *S. chinensis* exhibits antitumor [36], anti-hepatotoxic and hepatoprotective [37, 38], anti-cancer [39], neuroprotective [40], anti-diabetic [41], and antioxidant [39, 42] properties. Formation of nanoparticles using green chemistry, characterization, effects of fruit extracts and potential application in cancer medicine using *Schisandra* genus have been discussed in prior literature [34, 43-49].

The current therapeutic agents used for cancer treatment are very costly with additional problems such as severe side effects and toxicity on non-cancerous tissues. Consequently, it is necessary to explore a new cost-effective and biocompatible therapeutic approach against cancer.

For the above-mentioned reasons, the current study was designed to prepare and characterize the biosynthesized CuNPs using a bioreduction procedure with aqueous extract of *S. chinensis* as a bioreducing agent and evaluate its antiproliferative and apoptotic effects on A549 human lung cancer cell line (CRM-CCL-185TM), HT29 human colorectal adenocarcinoma cell line (ATCC® HTB-38TM) and MCF7 breast cancer cell line (ATCC® HTB-22TM).

MATERIALS AND METHODS

Materials

The dried *S. chinensis* berries extract was obtained from Gelinna Health Center (Xi'an Greena Biotech Co., Ltd., Yantra District., Xi'an, China); copper sulphate pentahydrate ($\text{CuSO}_4 \cdot 5\text{H}_2\text{O}$) used in the study was of analytical grade (Sigma-Aldrich); de-ionized and distilled water were directly obtained from our laboratory at the Universidad El Bosque, Bogotá D.C., Colombia; Dulbecco's Modified Eagle Medium (DMEM) culture medium, resazurin, dimethyl sulfoxide (DMSO) and all other used reagents and chemicals were purchased from Sigma-Aldrich; Fetal bovine serum (FBS) and Penicillin-Streptomycin solution was obtained from Gibco® Life Technologies and Trypsin-EDTA from Lonza.

Preparation of *S. chinensis* aqueous extract

20 g of the dried *S. chinensis* berries extract was taken in a beaker along with 100 mL of de-ionized water that it is heated at 60 °C during 30 minutes under reflux condi-

tions and cooled down to room temperature. After that the solution was filtered using Whatman Grade 2 filter paper to eliminate non-soluble materials obtaining a clear solution. The filtrate was stored at 4 °C for further experiments.

Biosynthesis of copper nanoparticles

The biosynthesis of CuNPs was performed according to Usha *et al.* [20] with slight modifications. The *S. chinensis* aqueous extract (50 mL) was mixed with 200 mL of 1 mM aqueous copper sulphate pentahydrate solution under continuous stirring at 80 °C on a hot plate. The plant extract was mixed by slow drip with the copper solution for 4 h. After complete mixing of the plant extract and precursor the mixture was incubated at 31 °C for 24 h. A color change from yellow to brick brown was observed that indicated the formation of copper nanoparticles. The solution was then centrifuged at 6000 rpm for 30 min. followed by re-dispersion of the pellets in deionized water to remove any unwanted biological materials. This procedure was done three times. Finally, the pellets were filtrated and dried at 80 °C in an oven and stored in screw-capped vials under ambient conditions for further characterization and application.

Characterization of biosynthesized CuNPs

Synthesized copper nanoparticles were subjected to various characterization studies for identification of size and morphology as follows:

UV-Spectroscopy:

The reduction of copper sulphate to copper was monitored by recording UV-Vis spectrum of the reaction mixture after diluting a small aliquot of the sample with deionized water. The measurements were recorded on a Genesys -Thermo Scientific UV-Vis spectrometer (model 10S) operated in 200–800 nm wavelength.

FT-IR analysis of bio-mass before and after bio-reduction:

Fourier-transform infrared spectra of *S. chinensis* berries extract powder and the dried CuNPs were acquired in the range 4000 to 500 cm^{-1} with a Bruker - Alpha Platinum Infrared Spectrophotometer by ATR technique.

X-Ray diffraction (XRD) studies:

X-ray diffraction measurement of the *S. chinensis* reduced CuNPs was carried out using a powder X-ray diffractometer instrument (PANalytical Xpert Pro) in the angle range of 100-700 operated at a voltage of 40 kV and a current of 30 mA with $\text{CuK}\alpha$ radiation in a θ - 2θ configuration. The crystallite domain size was calculated by using Debye- Scherrer formula.

Scanning electron microscopy (SEM):

SEM micrographs of the *S. chinensis* reduced CuNPs were obtained using a SEM Tesca Vega 3 SB microscope.

Antiproliferative activity and apoptosis evaluation

The cytotoxic potential of CuNPs was evaluated *in vitro* on different cell lines such as described below:

Propagation and maintenance of cell lines

The cell lines used in these studies were A549 human lung cancer cell line (CRM-CCL-185™), HT29 human colorectal adenocarcinoma cell line (ATCC® HTB-38™) and MCF7 breast cancer cell line (ATCC® HTB-22™). All lines were maintained in DMEM with sodium pyruvate (1 mM), penicillin (100 UI/mL), streptomycin (100 µg/mL), and 10% of Fetal bovine serum (FBS). Cells were cultured in T-25 flasks at 37.0 °C, 5% CO₂ and 80% relative humidity, changing media at least twice a week.

Sample preparation

S. chinensis reduced CuNPs stock solution (50 mg/mL) was made in a DMSO-phosphate-buffered solution (PBS) (1:1) mix and five 1:2 serial dilutions starting with 100 µg/mL were prepared in culture media and added to the cells. *S. chinensis* aqueous extract, while CuSO₄·5H₂O solutions were used as controls. In all experiments, the final concentration of DMSO in the wells was below to 0.1%.

In-vitro cytotoxic essay

The cells were seeded in 96-well flat-bottom plates at a density of 20000 cells per well for HT-29 and 5000 for A549 and MCF-7. Once the cells adhered to the support, they were exposed to treatments for 72 h. The effect of the vehicle was evaluated in all tests. The cytotoxicity of CuNPs, CuSO₄·5H₂O and *S. chinensis* extract was evaluated by the resazurin reduction assay.

Resazurin reduction essay

Following the exposure times to the treatments, the medium was replaced by 100 µL of 44 µM resazurin; then, after 4 hours of incubation, the fluorescence emitted by the viable and/or metabolically active cells was quantified at an excitation wavelength of 535 nm and an emission of 595 nm using a TECAN GENios spectrofluorometer. Assays were performed over three independent weeks in triplicate. The results were reported in terms of percentages of viability with respect to the control without treatment.

Apoptosis assay

The induction of apoptosis was examined using the fluorescein isothiocyanate (FITC) Annexin V Apoptosis Detection Kit with 7-AAD (BioLegend Inc., San Diego, USA) following the manufacturer's instructions. After treatment, attached cells were collected by trypsinization and washed with PBS, cell pellet obtained was resuspended in 50 μL of 1x annexin V binding buffer and incubated for 15 min at room temperature in the presence of 2 μL of annexin V-FITC and 2 μL of 7-AAD. After incubation, 200 μL of 1x annexin V binding buffer was added, and the percentage of apoptotic cells was analyzed using a BD Accuri™ C6 flow cytometer (BD Biosciences, San Jose, USA) and the FlowJo software (TreeStar, Inc). For each sample, 10000 total events were acquired. All experiments were conducted in triplicated, and cells treated with 100 nM of paclitaxel were included as death control.

Statistical analysis

All data were analyzed using Prism Software version 9.5 (GraphPad Software Inc., La Jolla, CA, USA). Statistical significance was determined using the *T*-test to compare two independent groups. Differences were considered significant at $p < 0.05$.

RESULTS AND DISCUSSION

UV-Vis Analysis spectra

The UV-Vis spectrum conducted on the aqueous dispersion of copper nanoparticles synthesized from the extract of *S. chinensis* showed a peak of maximum absorption at 475 nm as illustrated in Fig. 1. The solution exhibited a greenish-brown coloration after the reaction, which is consistent with previous reports confirming the production of nanoparticulate material [50]. The maximum absorption peak corresponds to the Surface Plasmon Resonance (SPR). Its position in this spectrum scale depends on various factors, such as the particle shape, size, the solvent used, and the general synthesis conditions, including factors like agitation and temperature, among others. However, absorption in this region of the UV spectrum confirms the formation of the metallic nanoparticles [51].

Infra Red Analysis spectra

During the bioreduction process, organic molecules lead to the formation of metallic nanoparticles. Consequently, the organic functional groups of the stabilizing molecules can be observed through infrared spectra. The infrared spectrum reveals various organic functional groups. In our case, the obtained nanoparticles were analyzed using

the FTIR (Fourier Transform Infrared) technique, and the results were compared with the spectrum of the dried sample of the pure aqueous extract of *S. chinensis*. The FTIR spectrum (ν_{\max} (cm^{-1})) of aqueous *S. chinensis* extract showed many characteristics absorption bands, namely at 3308 cm^{-1} (ν_{OH} , s, broad, polyhydroxyl hydrogen bonding), 2928 cm^{-1} (ν_{CH} , H_3CO , m), 1710 cm^{-1} ($\nu_{\text{C=O}}$, C=O , s), 1528 cm^{-1} ($\nu_{\text{C-C aromatic}}$, C-C- aromatic, m), 1406 cm^{-1} ($\nu_{\text{C-N}}$, amide, s), 1246 cm^{-1} ($\nu_{\text{C-O}}$, phenolic, s), 1029 cm^{-1} ($\nu_{\text{C-O}}$, ether, s) and 936 cm^{-1} ($\nu_{\text{C-H}}$, alkene, s); whereas, the synthesized nanoparticles at 3302 cm^{-1} (ν_{OH} , s, broad, polyhydroxyl hydrogen bonding), 2914 cm^{-1} (ν_{CH} , H_3CO , m), 1582 cm^{-1} ($\nu_{\text{C-C aromatic}}$, C-C aromatic, m), 1371 cm^{-1} ($\nu_{\text{C-N}}$, amide, m), 1025 cm^{-1} ($\nu_{\text{C-O}}$, ether, s) and 613 cm^{-1} ($\nu_{\text{C-H aromatic}}$, C-H- aromatic, s), as can be seen in figures 2 and 3.

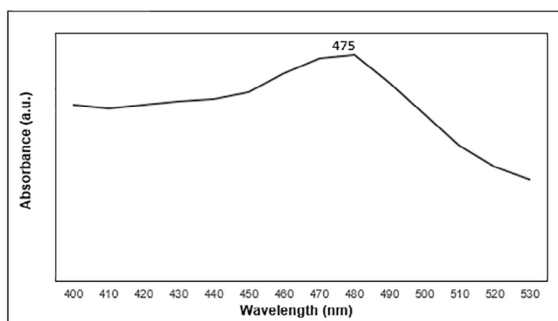


Figure 1. The UV spectrum of the nanoparticle dispersion.

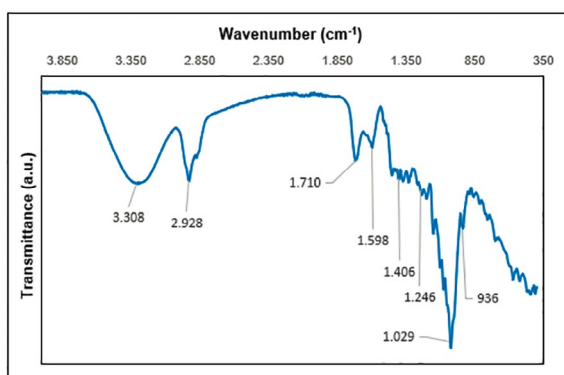


Figure 2. FTIR spectrum of *S. chinensis* aqueous extract

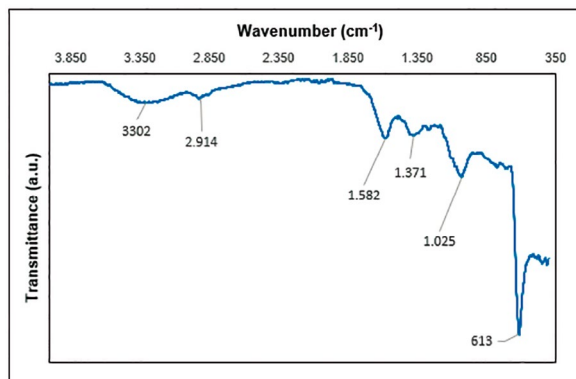


Figure 3. FTIR spectrum of copper nanoparticles

The infrared spectra of both the aqueous extract of *S. chinensis* and the formed nanoparticles display the characteristic functional organic groups found in the most abundant secondary metabolites of plant species, such as lignans [52]. The spectra confirm the presence of organic reducing groups that could exert dual function: on the one hand, the bioreduction of the metallic substrate, and, on the other hand, the stabilization of the formed nanoparticles.

X-Ray diffraction spectrum analysis

The crystallinity and crystallite size of copper nanoparticles synthesized were confirmed by XRD analysis as shown in Fig. 4 (red line).

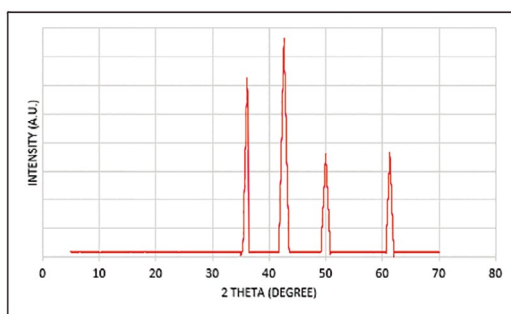


Figure 4. XRD pattern of copper nanoparticles

XRD spectrum showed distinct diffraction peaks at $2\theta = 36.12^\circ$, 42.6° , 50° and 61.3° . The crystallite size and crystallinity of copper nanoparticles synthesized from the aqueous extract of *S. Chinensis* were calculated according to the modified Scherrer equation

[53-55]. The crystallite size and crystallinity were found around 263.6 Å under the described experimental conditions, which indicates a high surface area and also a surface area/volume ratio of these nanoparticles.

Scanning electron microscopy (SEM)

Scanning Electron Microscopy allowed the observation of the surface morphology of nanoparticles. The SEM study demonstrated that size was around 26 nm, as could be inferred from the X-ray diffraction studies. In Fig. 5, spherical nanoparticles can be observed, along with some agglomerations, which possibly result from electrostatic interactions or hydrogen bonding between the different functional groups of the organic molecules that make up the coating of the generated nanoparticles.

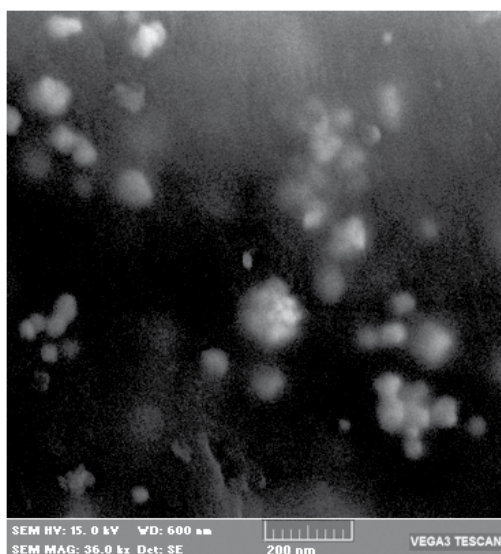


Figure 5. SEM image showing copper nanoparticles

Antiproliferative activity and apoptosis evaluation

The *in vitro* antiproliferative activity of reduced CuNPs, $\text{CuSO}_4 \cdot 5\text{H}_2\text{O}$ and *S. chinensis* extract was evaluated in lung cancer cells (A549), colon cancer cells (HT-29) and breast cancer cells (MCF-7) using the resazurin reduction assay, which is based on the ability of viable and metabolically active cells to reduce resazurin to resorufin. The results are shown in Fig. 6 and suggest that *S. chinensis* reduced CuNPs induce cytotoxic effects on all cancer cells in a dose-dependent manner, with 50 and 100 $\mu\text{g}/\text{mL}$ being the most effective concentrations at 72 h post-treatment. Interestingly, $\text{CuSO}_4 \cdot 5\text{H}_2\text{O}$ and extract does not affect the cell viability of tumor cell; in this way, only a moder-

ate reduction of cell viability was observed in HT-29 cells at the highest concentration tested. When the cell viability was compared, highly significant differences ($p \leq 0.0001$) between the three treatments in all tumor cell lines at the highest concentrations tested, were observed. On the other hand, calculated IC₅₀ values showed that HT-29 (IC₅₀ = 42.64 $\mu\text{g}/\text{mL}$) and MCF-7 cells (IC₅₀ = 40.68) were the most sensitive in comparison with A549 cells (IC₅₀ = 63.78) to treatment with CuNPs.

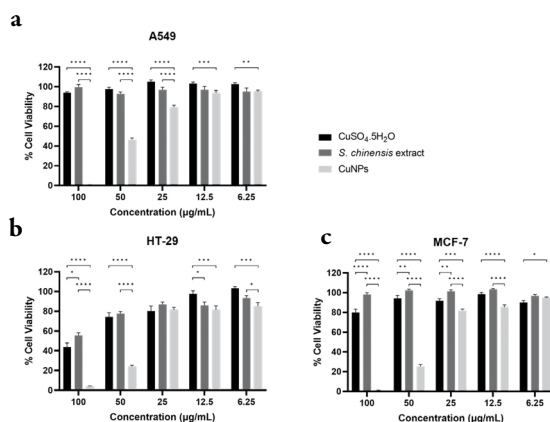


Figure 6. *S. chinensis* reduced CuNPs decreases cell viability of cancer cells in a dose-dependent manner. Three cancer cell lines (a) A549 (b) HT-29 and (c) MCF-7 were treated with different concentrations of CuNPs by 72 h. $\text{CuSO}_4 \cdot 5\text{H}_2\text{O}$ and *S. chinensis* extract were used as controls. Cells were incubated for 4 h after treatments with resazurin 44 μM , the fluorescence of each well was recorded using a spectrofluorometer ($\lambda_{\text{ex}} = 535 \text{ nm}$ and $\lambda_{\text{em}} = 595 \text{ nm}$) and percent viability was calculated using the fluorescence of untreated wells as 100%. The results are shown as the means \pm standard error of the mean (SEM) from three independent experiments conducted in triplicate. (*) $p \leq 0.05$, (**) $p \leq 0.01$, (***) $p \leq 0.001$, (****) $p \leq 0.0001$.

The resazurin assay measures changes in the redox metabolism that indicate a decrease in the cellular proliferation/viability, although they do not distinguish between the types of cellular death. For this reason, the presence of apoptotic cells through an annexin-V binding assay by flow cytometry was analyzed. As shown in Fig. 7, more than 80% of CuNPs-treated cells at the highest concentrations (100 or 50 $\mu\text{g}/\text{mL}$) were annexin-V positive, except for A549, on which a high level of apoptosis was induced at 100 $\mu\text{g}/\text{mL}$ (Fig. 7a). Similarly, a high proportion of death cell was only detected in HT-29 and MCF-7 cells treated with 100 $\mu\text{g}/\text{mL}$ of $\text{CuSO}_4 \cdot 5\text{H}_2\text{O}$ (81.7% and 92.3%, respectively; Figs. 7b and 7c); however, significant differences in apoptosis induction

between treatments were found at different concentrations. The percentage of A549 cells binding annexin-V was significantly higher in cultures treated with 100 $\mu\text{g}/\text{mL}$ of CuNPs in comparison with those treated with $\text{CuSO}_4 \cdot 5\text{H}_2\text{O}$ at the same concentration (90.5% versus 39.5%, respectively; $p \leq 0.01$; Fig. 7a). Interestingly, this difference was also observed in HT-29 and MCF-7 cells at a lower concentration. As shown in Figs. 7b and 7c, apoptosis induction on these cells was significantly enhanced after treatment with CuNPs 50 $\mu\text{g}/\text{mL}$ compared to $\text{CuSO}_4 \cdot 5\text{H}_2\text{O}$ at the same concentration (82.1% and 93.7% versus 22.2% and 10.2%, respectively; $p \leq 0.0001$). In contrast, the *S. chinensis* aqueous extract did not induce significant apoptotic cell death in any of the tested cells.

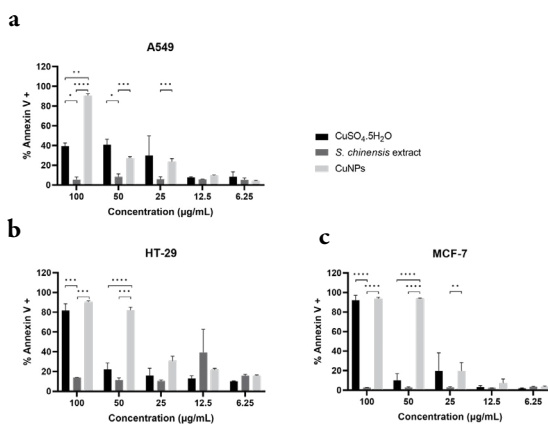


Figure 7. Apoptosis induction by *S. chinensis* reduced CuNPs in cancer cell lines. Three cancer cell lines (a) A549 (b) HT-29 and (c) MCF-7 were treated with different concentrations of CuNPs by 72 h and the apoptotic cells were identified analyzing the annexin-V binding to cell surface by flow cytometry. $\text{CuSO}_4 \cdot 5\text{H}_2\text{O}$ and *S. chinensis* extract were used as controls. The results are shown as the means \pm SEM from three independent experiments conducted in triplicate. (*) $p \leq 0.05$, (**) $p \leq 0.01$, (***) $p \leq 0.001$, (****) $p \leq 0.0001$.

To determine the percentage of early and late apoptotic cells in CuNPs-exposed cultures, flow cytometry was performed now using annexin-V and 7AAD. Early apoptotic cells showed annexin V+/7AAD– staining patterns, whereas late apoptotic cells exhibited annexin V+/7AAD+ staining patterns due to a loss of cell membrane integrity. In non-treated control cells, 3.79% of the A549 cells, 7.77% of the HT-29 cells and 2.90% of the MCF-7 cells were in early apoptosis, whereas 1.44%, 3.08% and 1.44% of the A549, HT-29 and MCF-7 cells, respectively, were in late apoptosis (Fig. 8). Simi-

lar results were obtained using *S. chinensis* extract, but exposition to $\text{CuSO}_4 \cdot 5\text{H}_2\text{O}$ resulted in a slightly higher early and late apoptosis processes. In contrast, after exposure to CuNPs, a significant increase of both apoptotic stages was identified within all cell cultures. Thus, 16.0% of the A549 cells, 17.9% of the HT-29 cells and 13.1% of the MCF-7 cells were in early apoptosis, whereas 76.6%, 61.1% and 81.2% of the A549, HT-29 and MCF-7 cells, respectively, were in late apoptosis. In contrast, a very low percentage of cells were in necrosis (annexin V-/7AAD+). All these results suggest that the *S. chinensis* reduced CuNPs were able to induce mainly early apoptotic cell death in cancer cells in a concentration-dependent manner.

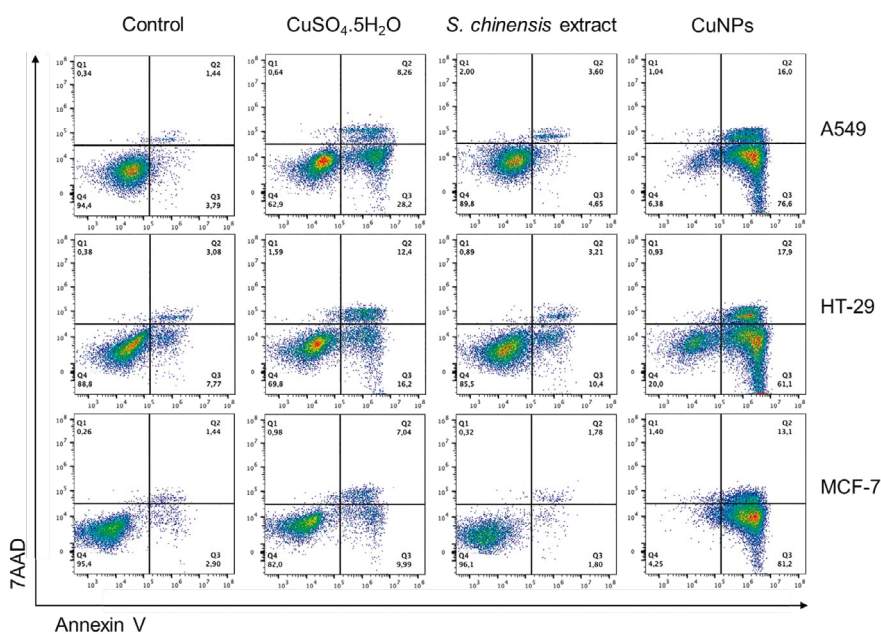


Figure 8. Early apoptosis was detected in A549, HT-29 and MCF-7 cells treated with *S. chinensis* reduced CuNPs. After a 72 h treatment with 100 $\mu\text{g}/\text{mL}$ (A549) or 50 $\mu\text{g}/\text{mL}$ (HT-29 and MCF-7) of $\text{CuSO}_4 \cdot 5\text{H}_2\text{O}$, *S. chinensis* extract or CuNPs, cells were stained with FITC annexin-V and 7-AAD. The percentage of annexin-V and/or 7-AAD positive cells was analyzed by flow cytometry. Dot plots from one representative of three independent experiments are shown. The control column represents cells without treatment.

CONCLUSIONS

Copper nanoparticles (CuNPs) were synthesized using a green synthesis method from the aqueous extract of *Schisandra chinensis* fruits. The obtained nanoparticles were characterized through spectroscopic methods, revealing a uniform particle size of approximately 26 nm. These nanoparticles were tested against three different tumor cell lines. Results suggest that the *S. chinensis* reduced CuNPs were able to induce mainly early apoptotic cell death in cancer cells in a concentration-dependent manner.

ACKNOWLEDGMENTS

We would like to express our gratitude to the Facultad de Ciencias – Universidad El Bosque (Bogotá D.C., Colombia), specifically the Department of Pharmaceutical Chemistry, and the Facultad de Ciencias – Universidad Nacional de Colombia (Bogotá D.C., Colombia), particularly the Department of Physics, for their technical support in providing reagents and materials, as well as for making their facilities and equipment available for the development of this research.

CONFLICTS OF INTEREST

The authors declare no conflict of interest.

REFERENCES

1. S. Panigrahi, S. Kundu, S.K. Ghosh, S. Nath, T. Pal, General method of synthesis for metal nanoparticles, *Journal of Nanoparticle Research*, **6**(4), 411-414 (2004). Doi: <https://doi.org/10.1007/S11051-004-6575-2>
2. A. Tamilvanan, K. Balamurugan, K. Ponappa, B.M. Kumar, Copper nanoparticles: Synthetic strategies, properties and multifunctional application, *International Journal of Nanoscience*, **13**(2), 1430001 (2014). Doi: <https://doi.org/10.1142/S0219581X14300016>
3. M.I. Din, R. Rehan, Synthesis, characterization, and applications of copper nanoparticles, *Analytical Letters*, **50**(1), 50-62 (2017). Doi: <https://doi.org/10.1080/00032719.2016.1172081>

4. M. Raffi, S. Mehrwan, T.M. Bhatti, J.I. Akhter, A. Hameed, W. Yawar, M.M.u. Hasan, Investigations into the antibacterial behavior of copper nanoparticles against *Escherichia coli*, *Annals of Microbiology*, **60**(1), 75-80 (2010). Doi: <https://doi.org/10.1007/s13213-010-0015-6>
5. E. Sizova, S. Miroshnikov, V. Polyakova, N. Gluschenko, A. Skalny, Copper nanoparticles as modulators of apoptosis and structural changes in tissues, *Journal of Biomaterials and Nanobiotechnology*, **3**, 97-104 (2012). Doi: <https://doi.org/10.4236/jbnt.2012.31013>
6. P. Fakhri, B. Jaleh, M. Nasrollahzadeh, Synthesis and characterization of copper nanoparticles supported on reduced graphene oxide as a highly active and recyclable catalyst for the synthesis of formamides and primary amines, *Journal of Molecular Catalysis A: Chemical*, **383-384**, 17-22 (2014). Doi: <https://doi.org/10.1016/j.molcata.2013.10.027>
7. N. Nagar, V. Devra, Green synthesis and characterization of copper nanoparticles using *Azadirachta indica* leaves, *Materials Chemistry and Physics*, **213**, 44-51 (2018). Doi: <https://doi.org/10.1016/j.matchemphys.2018.04.007>
8. S.S. Joshi, S.F. Patil, V. Iyer, S. Mahumuni, Radiation induced synthesis and characterization of copper nanoparticles, *Nanostructured Materials*, **10**(7), 1135-1144 (1998). Doi: [https://doi.org/10.1016/S0965-9773\(98\)00153-6](https://doi.org/10.1016/S0965-9773(98)00153-6)
9. S. Chandra, A. Kumar, P.K. Tomar, Synthesis and characterization of copper nanoparticles by reducing agent, *Journal of Saudi Chemical Society*, **18**(2), 149-153 (2014). Doi: <https://doi.org/10.1016/j.jscs.2011.06.009>
10. P.K. Khanna, S. Gaikwad, P.V. Adhyapak, N. Singh, R. Marimuthu, Synthesis and characterization of copper nanoparticles, *Materials Letters*, **61**(25), 4711-4714 (2007). Doi: <https://doi.org/10.1016/j.matlet.2007.03.014>
11. L. Zhou, S. Wang, H. Ma, S. Ma, D. Xu, Y. Guo, Size-controlled synthesis of copper nanoparticles in supercritical water, *Chemical Engineering Research and Design*, **98**, 36-43 (2015). Doi: <https://doi.org/10.1016/j.cherd.2015.04.004>
12. N.A. Dhas, C.P. Raj, A. Gedanken, Synthesis, characterization and properties of metallic copper nanoparticles, *Chemistry of Materials*, **10**(5), 1446-1452 (1998). Doi: <https://doi.org/10.1021/cm9708269>

13. B. Khodashenas, H.R. Ghorbani, Synthesis of copper nanoparticles: An overview of the various methods, *Korean Journal of Chemical Engineering*, **31**(7), 1105-1109 (2014). Doi: <https://doi.org/10.1007/S11814-014-0127-Y>
14. I. Hussain, N.B. Singh, A. Singh, H. Singh, S.C. Singh, Green synthesis of nanoparticles and its potential application, *Biotechnology Letters*, **38**(4), 545-560 (2015). Doi: <https://doi.org/10.1007/S10529-015-2026-7>
15. A. Gour, N.K. Jain, Advances in green synthesis of nanoparticles, *Artificial Cells, Nanomedicine, and Biotechnology*, **47**(1), 844-851 (2019). Doi: <https://doi.org/10.1080/21691401.2019.1577878>
16. K. Parveen, V. Banse, L. Ledwani, Green synthesis of nanoparticles: Their advantages and disadvantages, *AIP Conference Procedures*, **1724**(1), 020048 (2016). Doi: <https://doi.org/10.1063/1.4945168>
17. M.I. Din, F. Arshad, Z. Hussain, M. Mukhtar, Green adeptness in the synthesis and stabilization of copper nanoparticles: Catalytic, antibacterial, cytotoxicity, and antioxidant activities, *Nanoscale Research Letters*, **12**(1), 638 (2017). Doi: <https://doi.org/10.1186/s11671-017-2399-8>
18. A.H. Keihan, H. Veisi, H. Veasi, Green synthesis and characterization of spherical copper nanoparticles as organometallic antibacterial agent, *Applied Organometallic Chemistry*, **31**(7), e3642 (2017). Doi: <https://doi.org/10.1002/aoc.3642>
19. A.T. Joseph, P. Prakash, S.S. Narvi, Phytofabrication and characterization of copper nanoparticles using *Allium sativum* and its antibacterial activity, *International Journal of Science, Engineering and Technology*, **4**(2), 463-472 (2016). URL: <https://www.ijset.in/wp-content/uploads/2016/05/10.2348.ijset03160463.pdf>
20. S. Usha, K.T. Ramappa, S. Hiregoudar, G.D. Vasanthkumar, D.S. Aswatharayana, Biosynthesis and characterization of copper nanoparticles from tulasi (*Ocimum sanctum* L.) leaves, *International Journal of Current Microbiology and Applied Sciences*, **6**(11), 2219-2228 (2017). Doi: <https://doi.org/10.20546/ijc-mas.2017.611.263>
21. K. Ebrahimi, S. Shiravand, H. Mahmoudvand, Biosynthesis of copper nanoparticles using aqueous extract of *Capparis spinosa* fruit and investigation of its antibacterial activity, *Marmara Pharmaceutical Journal*, **21**(4), 866-871 (2017). URL: <https://dergipark.org.tr/en/download/article-file/407366>

22. M.W. Amer, A.M. Awwad, Green synthesis of copper nanoparticles by *Citrus limon* fruits extract, characterization and antibacterial activity, *Chemistry International*, **7**(1), 1-8 (2020). Doi: <https://doi.org/10.5281/zenodo.4017993>
23. N. Jayarambabu, A. Akshaykranth, T. Venkatappa-Rao, K. Venkateswara-Rao, R. Rakesh-Kumar, Green synthesis of Cu nanoparticles using *Curcuma longa* extract and their application in antimicrobial activity, *Materials Letters*, **259**, 126813 (2020). Doi: <https://doi.org/10.1016/j.matlet.2019.126813>
24. H.J. Lee, J.Y. Song, B.S. Kim, Biological synthesis of copper nanoparticles using *Magnolia kobus* leaf extract and their antibacterial activity, *Journal of Chemical Technology and Biotechnology*, **88**(11), 1971-1977 (2013). Doi: <https://doi.org/10.1002/JCTB.4052>
25. S. Kirubandanan, V. Subha, S. Renganathan, Green synthesis of copper nanoparticles using methanol extract of *Passiflora foetida* and its drug delivery applications, *International Journal of Green Chemistry*, **3**(2), 31-52 (2017). URL: <https://chemical.journalspub.info/index.php?journal=IJGC&page=article&cop=view&path%5B%5D=399>
26. S. Amaliyah, D.P. Pangesti, M. Masruri, A. Sabarudin, S.B. Sumitro, Green synthesis and characterization of copper nanoparticles using *Piper retrofractum* Vahl extract as bioreductor and capping agent, *Heliyon*, **6**(8), e04636 (2020). Doi: <https://doi.org/10.1016/j.heliyon.2020.e04636>
27. P.N. Padma, S.T. Banu, S.C. Kumari, Studies on green synthesis of copper nanoparticles using *Punica granatum*, *Annual Research & Review in Biology*, **23**(1), 1-10 (2018). Doi: <https://doi.org/10.9734/arrb/2018/38894>
28. S. Thakur, S. Sharma, S. Thakur, R. Radheshyam, Green synthesis of copper nano-particles using *Asparagus adscendens* roxb. Root and leaf extract and their antimicrobial activities, *International Journal of Current Microbiology and Applied Sciences*, **7**(4), 683-694 (2018). Doi: <https://doi.org/10.20546/ijc-mas.2018.704.077>
29. R.M. Kiriyanthan, S.A. Sharmili, R. Balaji, S. Jayashree, S. Mahboob, K.A. Al-Ghanim, F. Al-Misned, Z. Ahmed, M. Govindarajan, B. Vaseeharan, Photocatalytic, antiproliferative and antimicrobial properties of copper nanoparticles synthesized using *Manilkara zapota* leaf extract: A photodynamic approach, *Photodiagnosis and Photodynamic Therapy*, **32**, 102058 (2020). Doi: <https://doi.org/10.1016/j.pdpdt.2020.102058>

30. P. Kachesova, I. Goroshinskaya, V. Borodulin, The effect of copper nanoparticles on the progression of tumor *in vivo*, *Journal of Clinical Oncology*, **31**(15), 3084-3084 (2013). Doi: https://doi.org/10.1200/jco.2013.31.15_suppl.3084
31. D. Bharathi, R. Ranjithkumar, B. Chandarshekar, V. Bhuvaneshwari, Bio-inspired synthesis of chitosan/copper oxide nanocomposite using rutin and their anti-proliferative activity in human lung cancer cells, *International Journal of Biological Macromolecules*, **141**, 476-483 (2019). Doi: <https://doi.org/10.1016/j.ijbiomac.2019.08.235>
32. E. Halevas, A. Pantazaki, Copper nanoparticles as therapeutic anticancer agents, *Nanomedicine and Nanotechnology Journal*, **2**(1), 119 (2018). URL: <https://www.scientificliterature.org/Nanomedicine/Nanomedicine-18-119.pdf>
33. K.M. Metz, S.E. Sanders, J.P. Pender, M.R. Dix, D.T. Hinds, S.J. Quinn, A.D. Ward, P. Duffy, R.J. Cullen, P.E. Colavita, Green synthesis of metal nanoparticles via natural extracts: The biogenic nanoparticle corona and its effects on reactivity, *ACS Sustainable Chemistry & Engineering*, **3**(7), 1610-1617 (2015). Doi: <https://doi.org/10.1021/acssuschemeng.5b00304>
34. H. Du, X. Tan, Z. Li, H. Dong, L. Su, Z. He, Q. Ma, S. Dong, M. Ramachandran, J. Liu, L. Cao, Effects of *Schisandra chinensis* polysaccharide-conjugated selenium nanoparticles on intestinal injury in mice, *Animals*, **13**(5), 930 (2023). Doi: <https://doi.org/10.3390/ani13050930>
35. A. Szopa, R. Ekiert, H. Ekiert, Current knowledge of *Schisandra chinensis* (Turcz.) Baill. (Chinese magnolia vine) as a medicinal plant species: a review on the bioactive components, pharmacological properties, analytical and biotechnological studies, *Phytochemistry Reviews*, **16**(2), 195-218 (2017). Doi: <https://doi.org/10.1007/S11101-016-9470-4>
36. T. Zhao, G. Mao, M. Zhang, Y. Zou, W. Feng, X. Gu, Y. Zhu, R. Mao, L. Yang, X. Wu, Enhanced antitumor and reduced toxicity effect of *Schisanrae* polysaccharide in 5-Fu treated Heps-bearing mice, *International Journal of Biological Macromolecules*, **63**, 114-118 (2014). Doi: <https://doi.org/10.1016/j.ijbiomac.2013.10.037>
37. W. Li, X.N. Qu, Y. Han, S.W. Zheng, J. Wang, Y.P. Wang, Ameliorative effects of 5-hydroxymethyl-2-furfural (5-HMF) from *Schisandra chinensis* on alcoholic liver oxidative injury in mice, *International Journal of Molecular Sciences*, **16**(2), 2446 (2015). Doi: <https://doi.org/10.3390/IJMS16022446>

38. O. Wang, Q. Cheng, J. Liu, Y. Wang, L. Zhao, F. Zhou, B. Ji, Hepatoprotective effect of *Schisandra chinensis* (Turcz.) Baill. lignans and its formula with *Rubus idaeus* on chronic alcohol-induced liver injury in mice, *Food & Function*, **5**(11), 3018-3025 (2014). Doi: <https://doi.org/10.1039/C4FO00550C>
39. L. Zhang, H. Chen, J. Tian, S. Chen, Antioxidant and anti-proliferative activities of five compounds from *Schisandra chinensis* fruit, *Industrial Crops and Products*, **50**, 690-693 (2013). Doi: <https://doi.org/10.1016/j.indcrop.2013.08.044>
40. E.J. Jeong, H.K. Lee, K.Y. Lee, B.J. Jeon, D.H. Kim, J.-H. Park, J.-H. Song, J. Huh, J.-H. Lee, S.H. Sung, The effects of lignan-riched extract of *Schisandra chinensis* on amyloid- β -induced cognitive impairment and neurotoxicity in the cortex and hippocampus of mouse, *Journal of Ethnopharmacology*, **146**(1), 347-354 (2013). Doi: <https://doi.org/10.1016/J.JEP.2013.01.003>
41. H. Liu, C. Wu, S. Wang, S. Gao, J. Liu, Z. Dong, B. Zhang, M. Liu, X. Sun, P. Guo, Extracts and lignans of *Schisandra chinensis* fruit alter lipid and glucose metabolism *in vivo* and *in vitro*, *Journal of Functional Foods*, **19**(Part A), 296-307 (2015). Doi: <https://doi.org/10.1016/J.JFF.2015.09.049>
42. M.K. Kim, J.M. Lee, J.S. Do, W.S. Bang, Antioxidant activities and quality characteristics of omija (*Schizandra chinensis* Baillon) cookies, *Food Science and Biotechnology*, **24**(3), 931-937 (2015). Doi: <https://doi.org/10.1007/S10068-015-0120-1>
43. K. Fu, H. Zhou, C. Wang, L. Gong, C. Ma, Y. Zhang, Y. Li, A review: Pharmacology and pharmacokinetics of Schisandrin A, *Phytotherapy Research*, **36**(6), 2375-2393 (2022). Doi: <https://doi.org/10.1002/PTR.7456>
44. F. Sa, B.J. Guo, S. Li, Z.J. Zhang, H.M. Chan, Y. Zheng, S.M.Y. Lee, Pharmacokinetic study and optimal formulation of new anti-parkinson natural compound schisantherin A, *Parkinson's Disease*, **2015**, 951361 (2015). Doi: <https://doi.org/10.1155/2015/951361>
45. X. Wang, X. Wang, H. Yao, C. Shen, K. Geng, H. Xie, A comprehensive review on Schisandrin and its pharmacological features, *Naunyn-Schmiedeberg's Archives of Pharmacology*, **397**, 783-794 (2024). Doi: <https://doi.org/10.1007/S00210-023-02687-Z>

46. J. Pei, Q. Lv, J. Han, X. Li, S. Jin, Y. Huang, S. Jin, H. Yuan, Schisandra lignans-loaded enteric nanoparticles: preparation, characterization, and *in vitro*–*in vivo* evaluation, *Journal of Drug Targeting*, **21**(2), 180-187 (2013). Doi: <https://doi.org/10.3109/1061186X.2012.737000>
47. M. Shno, W. Yang, G. Han, Protective effects on myocardial infarction model: delivery of schisandrin B using matrix metalloproteinase-sensitive peptide-modified, PEGylated lipid nanoparticles, *International Journal of Nanomedicine*, **12**, 7121-7130 (2017). doi: <https://doi.org/10.2147/IJN.S141549>
48. S.G. Balwe, A.A. Rokade, S.S. Park, Y.T. Jeong, Green synthesis and characterization of supported gold nanoparticles (Au@PS) from *Schisandra chinensis* fruit extract: An efficient and reusable catalyst for the synthesis of chromeno[2,3-d]pyrimidin-2-yl)phenol derivatives under solvent-free conditions, *Catalysis Communications*, **128**, 105703 (2019). Doi: <https://doi.org/10.1016/j.catcom.2019.05.010>
49. A. Chen, R. Hu, Self-assembly loading of *Schisandra chinensis* nanoparticles and its effect on the malignant biological behavior of ovarian cancer cells, *Science of Advanced Materials*, **15**(2), 243-255 (2023). Doi: <https://doi.org/10.1166/SAM.2023.4447>
50. I. Subhankari, P.L. Nayak, Synthesis of copper nanoparticles using *Syzygium aromaticum* (cloves) aqueous extract by using green chemistry, *World Journal of Nano Science & Technology*, **2**(1), 14-17 (2013). URL: [https://www.idosi.org/wjnst/2\(1\)13/4.pdf](https://www.idosi.org/wjnst/2(1)13/4.pdf)
51. M. Atarod, M. Nasrollahzadeh, S.M. Sajadi, Green synthesis of a Cu/reduced graphene oxide/Fe₃O₄ nanocomposite using *Euphorbia wallichii* leaf extract and its application as a recyclable and heterogeneous catalyst for the reduction of 4-nitrophenol and rhodamine B, *RSC Advances*, **5**(111), 91532-91543 (2015). Doi: <https://doi.org/10.1039/C5RA17269A>
52. C.-C. Chyau, Y.-B. Ker, C.-H. Chang, S.-H. Huang, H.-E. Wang, C.-C. Peng, R.Y. Peng, *Schisandra chinensis* peptidoglycan-assisted transmembrane transport of lignans uniquely altered the pharmacokinetic and pharmacodynamic mechanisms in human HepG2 cell model, *PLoS One*, **9**(1), e85165 (2014). Doi: <https://doi.org/10.1371/journal.pone.0085165>

53. M.S. Hossain, S. Ahmed, Sustainable synthesis of nano CuO from electronic waste (E-waste) cable: Evaluation of crystallite size via Scherrer equation, Williamson-Hall plot, Halder-Wagner model, Monshi-Scherrer model, size-strain plot, *Results in Engineering*, **20**, 101630 (2023). Doi: <https://doi.org/10.1016/j.rineng.2023.101630>
54. F.T.L. Muniz, M.A.R. Miranda, C. Morilla Dos Santos, J.M. Sasaki, The Scherrer equation and the dynamical theory of X-ray diffraction, *Acta Crystallographica Section A: Foundations and Advances*, **72**(3), 385-390 (2016). Doi: <https://doi.org/10.1107/s205327331600365x>
55. A. Monshi, M.R. Foroughi, M.R. Monshi, Modified Scherrer equation to estimate more accurately nano-crystallite size using XRD, *World Journal of Nano Science and Engineering*, **02**(03), 154-160 (2012). Doi: <https://doi.org/10.4236/wjnse.2012.23020>

HOW TO CITE THIS ARTICLE

D.A. Tinjacá, O.A. Almanza, F. Delgado, S.J. Morantes, M.C. Medina, P. Torres, E. Martinez, Preparation and characterization of copper nanoparticles of *Schisandra chinensis* and evaluation of its antiproliferative activity, *Rev. Colomb. Cienc. Quim. Farm.*, **53**(1), 244-265 (2024). <https://doi.org/10.15446/rcciquifa.v53n1.112982>